HHS Public Access

Author manuscript

Biochim Biophys Acta. Author manuscript; available in PMC 2018 January 01.

Published in final edited form as:

Biochim Biophys Acta. 2017 January ; 1865(1): 121–131. doi:10.1016/j.bbapap.2016.09.004.

Inhibition and conformational change of SERCA3b induced by Bcl-2

Asha Hewarathna, **Elena Dremina**, and **Christian Schöneich**[1]

Department of Pharmaceutical Chemistry, University of Kansas, 2095 Constant Avenue, Lawrence, KS 66047, U.S.A.

Abstract

An interaction of Bcl-2 with SERCA had been documented *in vitro* using the SERCA1a isoform isolated from rat skeletal muscle [Dremina, E. S., Sharov, V. S., Kumar, K., Azidi, A., Michaelis, E. K., Schöneich, C. (2004) *Biochem. J. 383* (361–370)]. Here, we demonstrate the interaction of Bcl-2 with the SERCA3b isoform both *in vitro* and in cell culture. *In vitro*, the interaction of Bcl-2 with SERCA3b was studied using Bcl-2Δ21, a truncated form of human Bcl-2, and microsomes isolated from SERCA3b-overexpressing HEK-293 cells. For these experiments, SERCA3b was quantified by a combination of amino acid analysis and Western blotting. We observed that Bcl-2Δ21 both inactivates SERCA3b and co-immunoprecipitates with SERCA3b. The incubation with Bcl-2Δ21 changes the distribution of SERCA3b during sucrose density gradient centrifugation, likely as the result of Bcl-2Δ21-induced conformational change of SERCA3b. When SERCA3b-overexpressing HEK-293 cells were co-transfected with Bcl-2, Bcl-2-dependent SERCA3b inactivation was observed. In these cells, Bcl-2 interaction with SERCA3b was demonstrated by co-immunoprecipitation. Furthermore, overexpression of Bcl-2 reduced fluorescein isothiocyanate (FITC) labeling of SERCA3b. Together, our data provide evidence for the interaction of Bcl-2 with SERCA3b *in vitro* and in cell culture, and for Bcl-2-dependent conformational and functional changes of SERCA3b.

Keywords

apoptosis; cancer; Bcl-2; SERCA; Ca^{2+}-ATPase; protein-protein interaction

1. Introduction

Apoptosis, programed cell death, is essential for the development and survival of multicellular organisms while impaired apoptosis contributes to several pathologies, including AIDS, Alzheimer's disease, Parkinson's disease and cancer [1]. One of the important parameters regulating pro- and anti-apoptotic processes is the intracellular Ca^{2+}

[1]Author for correspondence Department of Pharmaceutical Chemistry, University of Kansas, 2095 Constant Avenue, Lawrence, KS 66047, U.S.A., schoneic@ku.edu.

concentration, $[Ca^{2+}]_i$ [2]. A precisely controlled $[Ca^{2+}]_i$ is essential to maintain Ca^{2+} homeostasis in cells. Resting levels of cytosolic free Ca^{2+} are maintained at ~100 nM, maintained through active transport of Ca^{2+} from the cytosol to the extracellular space (~1.2 mM free Ca^{2+}), and into intracellular compartments, such as mitochondria and the endoplasmic reticulum (ER) [3]. Ca^{2+} is released from the ER along its concentration gradient through the inositol trisphosphate receptor (IP3R) and the ryanodine receptor (RyR) [4]. Mitochondria, which are strategically located near the ER, modulate and synchronize Ca^{2+} signals [5, 6]. Ca^{2+} is recycled to the ER by reuptake of Ca^{2+} from the cytosol into the ER lumen through the sarco/endoplasmic reticulum Ca^{2+}-ATPase (SERCA), a Ca^{2+} pump, which utilizes ATP and maintains as high as 100–500 μM free Ca^{2+} within the ER lumen [7]. Three distinct genes encode three major SERCA isoforms in mammals: SERCA1, SERCA2, and SERCA3. Here, the SERCA3 isoform displays unique characteristics when compared to SERCA1 and SERCA2, such as a reduced apparent affinity for Ca^{2+}, inhibition by platelet intracellular membrane 430 (PL/IM430) antibody, and an optimal pH for enzyme activity of pH=7.2–7.4 [8, 9]. SERCA3 is always co-expressed with the ubiquitous SERCA2b isoform [10] but the physiological importance of the unique characteristics of SERCA3 have yet to be defined in detail.

SERCA3 is expressed in platelets, lymphoid cells, mast cells, endothelial cells, and epithelial cells [11, 12]. It displays the highest isoform diversity where alternative splicing of the SERCA3 gene generates six isoforms, SERCA3a, SERCA3b, SERCA3c, SERCA3d, SERCA3e and SERCA3f, which are different in their C-terminal regions [13]. The species-specific expression of SERCA3 produces five isoforms (3b–3f) in humans, two isoforms (3b and 3c) in mice, and one isoform (3b or 3c) in rats [13]. In contrast, SERCA3a expression is not species specific [14]. Members of the SERCA3 sub-family exhibit different enzyme activities; the protein of interest in this study, SERCA3b, displays the highest turnover rate among all SERCA3 isoforms [9].

Bcl-2, which is best known for its anti-apoptotic function, is a member of the Bcl-2 protein family, which comprises both pro-apoptotic and anti-apoptotic proteins, such as Bax, Bak and Bcl-xL respectively [15]. Bcl-2 can inhibit apoptosis by various pathways, including the interaction with pro-apoptotic family members [16, 17], regulation of Ca^{2+} homeostasis [18], the interaction with mitochondrial channels (e.g., the voltage-dependent anion channel, VDAC) [19, 20], the regulation of mitochondrial membrane permeability [21]. Bcl-2-dependent regulation of Ca^{2+} homeostasis may proceed via various mechanisms including the modulation of ER Ca^{2+} release and uptake. For example, the overexpression of Bcl-2 in HeLa cells decreased the steady-state Ca^{2+} concentration in the ER and the Golgi apparatus, which is determined by the equilibrium between active Ca^{2+} uptake and passive Ca^{2+} release, suggesting that either of these processes could be affected by Bcl-2 [22]. It was initially concluded that Bcl-2 overexpression increased the ER Ca^{2+} leakage [22]. However, Abeele et al. reported a depletion of ER Ca^{2+} content following Bcl-2 overexpression through both Ca^{2+} uptake and Ca^{2+} release mechanisms [23]. Overexpression of Bcl-2 in LNCaP prostate cancer cells inhibited the Ca^{2+} uptake by downregulation of the expression of SERCA2b and calreticulin [23]. Similarly, Bcl-2 reduced the ER Ca^{2+} content by increasing the Ca^{2+} permeability of the ER membrane, thereby promoting cell survival [24].

Bcl-2-mediated Ca^{2+} leakage and the reduction of ER Ca^{2+} content was also observed in Bcl-2-overexpressing MCF-7 breast cancer cells [25].

An alternative pathway for the Bcl-2-dependent regulation of ER Ca^{2+} involves the interaction of Bcl-2 with inositol 1,4,5-triphosphate receptors (IP3R) [26], where the BH4 domain of Bcl-2 interacts with a region in the regulatory and coupling domain of the IP3R [27]. Bcl-2 can reduce IP3R-dependent Ca^{2+} release to preserve the ER Ca^{2+} levels [28]. Bcl-2 appears to inhibit and enhance specific Ca^{2+}-dependent signals. For example, Bcl-2 can discriminate between Ca^{2+} signals and selectively inhibit high amplitude transient Ca^{2+} elevations that lead to cell death [29]. Moreover, Bcl-2 was proposed to convert apoptogenic high Ca^{2+} signals to pro-survival Ca^{2+} oscillations through various mechanisms, such as the direct interaction with IP3R, impaired phosphorylation of IP3R, or by reducing ER Ca^{2+} content [30, 31].

Another potential pathway by which Bcl-2 may modify ER Ca^{2+} levels is the modulation of SERCA activity [32]. *In vitro* Bcl-2 interacts with and inhibits SERCA1 and SERCA2b, associated with unfolding of SERCA and modification of FITC binding [32]. The interaction of Bcl-2 and SERCA is modulated by heat shock protein 70 (Hsp70) [33].

In the present study, we have evaluated the interaction of Bcl-2 with SERCA3b and extended these studies to cell culture. We observed that Bcl-2 interacts with and partially inhibits SERCA3b activity both *in vitro* and in cell culture. Further, the inhibition of SERCA3b correlates with a Bcl-2-dependent conformational change of SERCA3b.

2. Materials and methods

2.1. Materials

GE Healthcare Amersham Enhanced Chemiluminiscence (ECL) or ECL-Plus Chemiluminiscence detection kits were purchased from Fisher Scientific (Pittsburgh, PA). The anti-Bcl-2 antibody (sc-7382) and the PL/IM430 antibody were from Santa Cruz Biotechnology (Santa Cruz, CA). The anti-fluorescein/Oregon Green monoclonal antibody was obtained from Molecular Probes (Grand Island, NY). The Coomassie Plus protein assay, amino acid standard mixture, 6N HCl and secondary horseradish peroxidase-conjugated (HRP) anti-mouse antibodies were from Pierce (Rockford, IL). Precision Plus Protein Dual Color standards, Tris-glycine buffer, pH 7.5 and 4–20% Tris-HCl ready gels were purchased from Bio-Rad (Hercules, CA). Tris-glycine-SDS running buffer was from Life Science Products (Frederick, CO). The PVDF membrane (0.45 μm) was purchased from Millipore (Bedford, MA). EDTA-free protease inhibitor cocktail was from Roche Diagnostics (Indianapolis, IN). Isopropyl β-D-1-thiogalactopyranoside (IPTG) was obtained from AmericanBio, Inc. (Natick, MA). Glutathione S-transferase (GST) was obtained from GenScript USA Inc. (Piscataway, NJ). Partial recombinant protein of SERCA3 with a GST tag at N-terminal, ATP2A3, (catalog no. H00000489-Q01) was purchased from (Abnova, Taiwan). QuickChange multi site-directed mutagenesis kit and XL10-Gold ultracompetent cells were purchased from Stratagene (La Jolla, CA). Dulbecco's modified Eagle's medium (DMEM), Lipofectamine 2000 transfection reagent and SeeBlue Plus2 pre-stained standard were obtained from Invitrogen (Carlsbad, CA). Thrombin-binding beads, glutathione-

agarose beads, protein A-agarose beads, alanine and other chemicals were purchased from Sigma (St. Louis, MO).

2.2. G145E-Bcl-2 mutant construction, transformation, DNA isolation, and sequencing

The oligonucleotide primer of 5'-AGG GAC GGG GTG AAC TGG GAG AGG ATT GTG GCC TTC TTT GAG-3' for the G145E mutant of Bcl-2 was designed and purchased from DNA technologies, Inc. (Coralville, IA). Mutant DNA strands were synthesized using the QuickChange multi site-directed mutagenesis kit according to the protocol provided with the kit. The polymerase chain reaction (PCR) was carried out using a thermal cycler (MJ Mini personal thermal cycler, Bio-Rad Laboratories, Hercules, CA) according to the following program: one cycle of incubation at 95°C for 1 min followed by 30 cycles of incubation at 95°C for 1 min, 55°C for 1 min and 65°C for 10 min. The transformations of PCR products were done using XL10-Gold ultracompetent cells according to the manufacturer's protocol. Mutant plasmid DNA was isolated from a few colonies using the QIAGEN Plasmid mini kit according to the manufacturer's protocol and the isolated DNA samples were submitted for sequencing (Northwoods DNA, Inc., Solway, MN).

2.3. Cell culture and transfections

HEK-293 cells, which were stably transfected with a human SERCA3b-encoding vector were a kind gift of Dr. Jocelyne Enouf (INSERM, Villejuif, France). Cells were cultured in DMEM, supplemented with 10% bovine calf serum, 100 μg/mL penicillin streptomycin and 200 μg/mL geneticin at 37°C in a humidified 5% CO_2 atmosphere.

Cultures of *E. coli* cells that were transformed with plasmid DNA encoding either human Bcl-2, an empty vector (without the sequence for the human Bcl-2 gene), or G145E-Bcl-2 were used to grow bacteria in large scale and DNA was isolated using the QIAGEN Plasmid Plus Maxi Kit according to the manufacturer's protocol. HEK-293 cells (stably transfected with a human SERCA3b-encoding vector) were transiently co-transfected separately with either isolated Bcl-2 DNA, empty-vector DNA, or G145E-Bcl-2 DNA using the Lipofectamine 2000 transfection reagent according to the manufacturer's protocol. The cells were harvested 48 hrs after transfection and microsomes were isolated.

2.4. Microsome preparation

Microsomes were isolated according to previously published methods [34]. HEK-293 cells from five 10-cm dishes were scraped down in PBS/5 mM EDTA and spun down at 1,000×g for 3 min. The supernatant was discarded and the cells were swollen in 2 mL of lysis buffer (10 mM Tris HCl, pH 7.5, and 0.5 mM $MgCl_2$) for 10 min followed by the addition of phenylmethylsulfonyl fluoride (PMSF) (final concentration of 0.1 M) and aprotinin (final content of 100 U/mL). The cells were then lysed with 40 strokes using a Dounce homogenizer with a tight A pestle. 2 mL of a solution containing 0.5 M Sucrose, 10 mM Tris, pH 7.5, 40 μM $CaCl_2$, 6 mM β-mercaptoethanol and 0.3 M KCl were added, and cells were lysed again with additional 20 strokes. The resulting cellular homogenate was centrifuged at 8,000×g for 20 min and 0.9 mL of 2.5 M KCl were added to the supernatant, and the post-mitochondrial fraction, referred to as "microsomes" was separated by centrifugation at 100,000×g for 1 hr at 4°C using an SW41 rotor in a L90K ultracentrifuge

(Beckman Coulter, Fullerton, CA). Microsomes were resuspended in a solution containing 0.25 M sucrose, 10 mM Tris, pH 7.5, 20 μM $CaCl_2$, 3 mM β-ME and 0.15 M KCl, and the protein concentration was measured by Coomassie Plus protein assay. Microsomes were aliquoted and quickly frozen in liquid N_2 for storage at −70°C.

2.5. SDS-PAGE separation and Western blotting

Protein samples were separated on 4–20% Tris-HCl ready gels using a Tris-glycine-SDS running buffer. Precision Plus Protein Dual Color standards or SeeBlue Plus2 pre-stained standard were used as reference markers for the molecular weights of proteins. Following electrophoresis, the gels were either stained with Coomassie brilliant blue or transferred onto a PVDF membrane for Western blotting.

Western blotting was carried out according to a previously published protocol with some modifications [32]. Following SDS-PAGE, proteins were transferred onto a 0.45 μm PVDF membrane, which was pre-soaked with methanol and pre-washed with distilled water, at 100 V for 2 hrs using a Tris-glycine buffer, pH 7.5. The membrane was blocked with 5% (w/v) milk in 20 mM Tris, pH 7.5, 150 mM NaCl and 0.1% Tween 20 for 1 hr at room temperature, followed by treating with the desired antibodies for immunodetection. GE Healthcare Amersham Enhanced chemiluminiscence (ECL) or ECL-Plus chemiluminiscence detection kits were used to visualize the bands according to the manufacturer's protocol.

2.6. Expression and purification of Bcl-2Δ21

Bcl-2Δ21 was expressed as GST-Bcl-2Δ21 using a pGEX3T vector in *E. coli* as the host strain according to a previously established method [32]. 5 mL of the starter culture was used to inocculate one liter of Luria-Bertani (LB) medium, which was incubated at 37°C with vigorous shaking until the optical density reached 0.4–0.475 at 600 nm. Protein expression was induced by the addition of 0.12 g of IPTG, followed by 5 min cooling on ice. Next, the culture was grown at 32°C for 3–4 hrs with vigorous shaking. The bacterial culture was harvested by centrifugation at 6,000×g for 10 min. The pellet was resuspended in a buffer containing 7.5 mM Tris, pH 8, 150 mM NaCl, and 3 mM EDTA, followed by incubation with lysozyme (0.1 mg/mL) on ice for 15–25 min. Next, the mixture was sonicated in the presence of 5 mM DTT, 1 mM PMSF and 1.5% (w/v) Sarkosyl for 40 sec., followed by centrifugation at 10,000×g at 4°C for 45 min. The resulting supernatant was incubated with 500 μl of glutathione-agarose beads at 4°C for 3 hrs in the presence of 1% (v/v) Triton. The beads were then separated by centrifugation at 4,000×g for 5 min. Finally, the beads were washed and resuspended in a buffer containing 7.5 mM Tris, pH 8, 150 mM NaCl, and 3 mM EDTA, and incubated with thrombin (5 units) for 1 hr at room temperature. Finally, 20 μl of thrombin-binding beads were added to the mixture and the mixture was incubated at 4°C for 30 min to yield pure Bcl-2Δ21. Purified Bcl-2Δ21 was further analyzed by SDS-PAGE and Western blotting with mouse monoclonal anti-Bcl-2 antibody (sc-7382) to confirm Bcl-2Δ21 protein expression.

2.7. Co-immunoprecipitation of SERCA3b with Bcl-2Δ21 added to microsomes

Co-immunoprecipitation was performed using a previously described protocol [32]. Microsomes were incubated in 500 μl of buffer contained 50 mM Tris-HCl, pH 7.4, 10 mM

EDTA, 1% Nonidet P40, 1 mM PMSF and complete, EDTA-free protease inhibitor cocktail in the presence and absence of Bcl-2Δ21 for 1 hr at 37°C. First, preclearing was done by incubating protein mixtures with 30 μl of protein A-agarose beads at 4°C for 30 min, and then 1 μg of anti-Bcl-2 antibody or PL/IM430 antibody was added to the supernatant for incubation at 4°C for 2 hrs. Next, protein A-agarose beads were added, and the mixture was incubated at 4°C for 1 hr. The bead-bound immunocomplexes were isolated and separated by SDS-PAGE followed by Western blotting with the anti-Bcl-2 antibody and the PL/IM430 antibody as described above.

2.8. Co-immunoprecipitation of SERCA3b and Bcl-2 in microsomes of doubly transfected HEK-293 cells

The co-immunoprecipitation procedure described above was carried out for microsomes isolated from HEK-293 cells overexpressing only SERCA3b, and HEK-293 cells overexpressing both SERCA3b and Bcl-2.

2.9. Sucrose density gradient centrifugation

Sucrose density gradient fractionation of microsomal proteins was carried out according to previously described methods [32]. All sucrose solutions were prepared in MBS buffer (25 mM MES, pH 6.5, 150 mM NaCl, 5 mM EDTA and 1 mM PMSF). Microsomes (200μg in 300 μl) were mixed with 2 mL of 0.5 M Na_2CO_3 buffer, pH 11, and 2 mL of 90% sucrose solution and placed into the bottom of an ultracentrifuge tube. 4 mL of 38% and 5% sucrose solutions were also added in order to set a discontinuous sucrose gradient. The tubes were then ultracentrifugated at 130,000×g in a SW41 rotor (Beckman Coulter, Fullerton, CA) for 18 hrs at 4°C. Finally, 1-mL fractions were collected from top to bottom of the tube and the fractions were separated by SDS-PAGE and analyzed by Western blotting with the PL/IM430 antibody.

2.10. FITC labeling

FITC labeling of microsomal samples was done according to a protocol published earlier [35]. Microsomes (20 μg) isolated from cells overexpressing both SERCA3b and Bcl-2, and microsomes (20 μg) isolated from SERCA3b-encoding cells additionally transfected with the empty vector (control) were incubated with 50 mM Tris-HCl, pH 8.8, 250 mM Sucrose, 0.1 mM $CaCl_2$, 5 mM $MgCl_2$, 20 μM FITC and protease inhibitor for 1 hr at room temperature in the dark. The reaction was stopped by addition of 4X SDS sample buffer and the samples were separated by SDS-PAGE followed by Western blotting with the anti-fluorescein/Oregon Green monoclonal antibody. FITC levels were determined by densitometry.

2.11. Densitometry

After Western blotting, the developed X-ray films were scanned and densitometry was performed with the NIH ImageJ software (http://rsb.info.nih.gov/ij). Developed X-ray films were scanned and the scanned images were converted into 8-bit gray scale images. After background subtraction, a band was selected by drawing a rectangle and this was repeated

for each band of interest. The selected bands were plotted using the “analyze > gels > plot lanes” commands and the areas under the peaks were determined.

2.12. Characterization of SERCA3b

2.12.1. Ca^{2+}-ATPase activity of SERCA3b—Ca^{2+}-dependent ATPase activities of microsomes isolated from cells overexpressing only SERCA3b, cells overexpressing both SERCA3b and Bcl-2, cells overexpressing both SERCA3b and G145E-Bcl-2, and cells transfected with both the SERCA3b vector and an empty vector (as a control for Bcl-2 overexpression) were measured separately. For in vitro studies, microsomes isolated from SERCA3b overexpressing cells were incubated with or without Bcl-2Δ21 for 1 hr at 37°C prior to the ATP hydrolysis assay.

We used the assay reported by Chandrasekera et al., in which ATP hydrolysis is coupled to the oxidation of NADH, measured at 340 nm [36]. Microsomes were added to 150 μl of a reaction mixture containing 120 mM KCl, 25 mM MOPS, pH 7, 2 mM $MgCl_2$, 1 mM ATP, 1.5 mM phospho-enol-pyruvate, 1 mM DTT, 0.5 mM EGTA, 0.45 mM $CaCl_2$ ($[Ca^{2+}]_{free}$~3 μM), 0.32 mM NADH, 5 U/mL pyruvate kinase, 10 U/mL lactate dehydrogenase, and 2 μM calcium ionophore (A23187), and the decrease in absorbance at 340 nm was followed for 10 min at 37°C in a microplate spectrophotometer (SpectraMax plus 50–60 Hz, Molecular Devices, LLC, Sunnyvale, CA) [36]. The linear region of the trace was used to determine the enzyme activity and the Ca^{2+}-dependent ATPase activity was obtained by subtracting the activity in the presence of EGTA from the total activity in the presence of Ca^{2+}. The Ca-Mg-ATP-EGTA Calculator (http://maxchelator.stanford.edu/CaMgATPEGTA-NIST.htm) was used to calculate the free Ca^{2+} concentration, $[Ca^{2+}]_{free}$, in the assay solution when different amounts of Ca^{2+} were added.

The graph of Ca^{2+}-ATPase activity as a function of $\log[Ca^{2+}]_{free}$ was generated using Origin software. SigmaPlot software was used for non-linear curve fitting and kinetic parameter calculations. Data points were fit to an equation, which represents a cooperative model of the Michaelis-Menten equation to determine $K_{1/2}$,

$$\text{Enzyme rate} = v_{max}[Ca^{2+}]^n_{free} / K^n_{\frac{1}{2}} + [Ca^{2+}]^n_{free},$$

where v_{max} is the maximum activity, n is the Hill coefficient, and $K_{½}$ is the substrate concentration at half maximum of enzyme activity.

2.12.2. Quantification of SERCA3b in microsome preparations using densitometry and amino acid analysis—To quantify SERCA3b in isolated microsomes, we designed a protocol based on the absolute quantification of a reference standard, ATP2A3, which is a partial sequence of SERCA3 fused to a GST tag. The construct ATP2A3 contains a 1:1 stoichiometry of GST and the partial sequence of SERCA3b. Hence, absolute quantification of GST in ATP2A3 permits the absolute quantification of the partial sequence of SERCA3b.

For the absolute quantification of GST in ATP2A3, we first generated an independent GST standard using commercially available GST. In this standard, the GST concentration was determined by amino acid analysis, and subsequently a defined amount of GST was blotted on a PVDF membrane, and Western blot analysis was performed using an anti-GST antibody. This Western analysis served to create a response factor for subsequent quantification of ATP2A3 with the anti-GST antibody to generate a reference standard for the SERCA3b partial sequence in ATP2A3. A standard curve generated with known amounts of ATP2A3 was then used for Western blot quantitation of SERCA3b in isolated microsomes. The ATP2A3 mouse monoclonal antibody raised against partial recombinant ATP2A3, which recognizes SERCA3 proteins of human origin, was used as the primary antibody.

Densitometry analysis after Western blotting was carried out as explained above without background subtraction. The band with the highest peak area, which corresponds to the darkness and size of the band, was selected and the relative peak areas of all bands on Western blot were calculated relative to the selected band.

Amino acid analysis of GST was performed as previously described [37]. Protein samples were gas phase hydrolyzed with 6N HCl in the presence of 1% (w/v) phenol for 22 hrs at 110°C under vacuum. The resultant amino acids were derivatized using o-phthalaldehyde. Derivatized amino acids were analyzed by reversed-phase HPLC (Varian 9050) with UV detection (Varian 9050) at λ=335 nm, and the amounts of selected amino acids were calculated relative to a chosen amino acid standard. A mixture of amino acids as external calibration standards, along with alanine, was used in this analysis and the normalized peak area of alanine was used to construct a calibration curve. The amino acid separation conditions were as follows. The C-18 column (250 × 4.6 mm) was pre-heated to 35°C, and equilibrated with mobile phase A (95% 25 mM NaAc, pH 5.8 and 5% THF). The amino acid derivatives were eluted by a linear gradient changing mobile phase B (95% MeOH and 5% THF) in the following way with a flow rate of 0.7 mL/min: 5% to 15% within 0.5 min, 15% to 45% within 20 min, 45% to 90% within 40 min.

3. Results

3.1. Expression and quantification of SERCA3b

Microsomes isolated from human SERCA3b overexpressing HEK-293 cells were used as the source of human SERCA3b. The human SERCA3-specific PL/IM430 antibody was used to monitor human SERCA3b protein expression. Western blot analysis recognized a single band at ~100 kDa that corresponds to the theoretical molecular weight of SERCA3b (114 kDa) [38]. To quantify the content of SERCA3b in isolated microsomes, we selected as a reference ATP2A3, a commercially available partial sequence of SERCA3 fused to a GST tag. ATP2A3 represents a 353 amino acid construct with a molecular weight of 38.83 kDa, containing a sequence identical to the 501–621 amino acid sequence of SERCA3. A calibration curve generated with known amounts of GST was used to determine the GST content in ATP2A3, which was ~0.01±0.007 nmol per 1 μg of ATP2A3 (n=3). Accordingly, the content of SERCA3 in 1 μg of ATP2A3 is ~0.01±0.007 nmol. Subsequently, known amounts of ATP2A3 were used to generate a response factor for the PL/IM430 antibody to

quantify SERCA3b. For this, ATP2A3 and microsomal fractions from HEK-293 cells overexpressing SERCA3b were blotted side by side. Figure 1 shows a calibration curve obtained from an individual experiment using known amounts of ATP2A3, which was used to quantify SERCA3b in microsomal preparations. A series of dilutions of ATP2A3 was separated by SDS-PAGE alongside the microsomal proteins in three different experiments.

Through our calibration, we determined that the SERCA3b content is $(7\pm3)\times10^{-4}$ nmol per 1 μg of microsomal proteins isolated from SERCA3b overexpressing HEK-293 cells.

3.2. SERCA3b activity in transfected HEK-293 cells

Using a series of different added Ca^{2+} concentrations, the apparent affinity of SERCA3b for Ca^{2+} was determined as 1.57±0.19 μM and the Hill coefficient (n) as 1.04±0.13, by plotting ATPase activity vs. $[Ca^{2+}]_{free}$ (Figure 2). For reference, we also measured the Ca^{2+}-dependent activity of SERCA1a ($K_{1/2}$=0.52±0.05 μM, n=1.12±0.13), which is included in Figure 2 (open symbols). Our value for the apparent Ca^{2+} affinity of SERCA3b, 1.57±0.19 μM is in reasonable close agreement with reported values (1.1–1.8 μM) [8, 36, 39]. We note that the published Ca^{2+} affinity of SERCA3 was measured in different cell lines but was not assigned to a specific isoform of SERCA3. The effect of Bcl-2Δ21 on the apparent Ca^{2+} affinity of SERCA3b was demonstrated in Figure S1 and the exogenous addition of Bcl-2Δ21 did not significantly alter the apparent Ca^{2+} affinity, as previously observed for SERCA1.

3.3. The effect of Bcl-2Δ21 on the activity of SERCA3b in vitro

Microsomes containing SERCA3b were incubated with known amounts of Bcl-2Δ21 in order to test whether *in vitro* Bcl-2Δ21 had an effect on SERCA3b activity. Earlier, we had shown that Bcl-2Δ21 and full-length Bcl-2 had similar effects on SERCA1 *in vitro* [32]. The ATP hydrolysis activity of SERCA3b was assayed in the absence and presence of Bcl-2Δ21 at a molar ratio of SERCA3b:Bcl-2Δ21=3:2. The Ca^{2+}-ATPase activity at 0 min was measured immediately following the addition of Bcl-2Δ21 to the microsomes. Incubation of microsomes alone at 37°C resulted in a slight decrease of SERCA3b activity over time. The extent of SERCA3b inactivation was higher when Bcl-2Δ21 was added (Figure 3). In the presence of thapsigargin, a potent inhibitor of the SERCA family, complete inhibition of ATPase activity was observed, indicating that the measured ATP hydrolysis activity corresponds to SERCA activity.

3.4. Co-immunoprecipitation of SERCA3b with Bcl-2Δ21 in vitro

Co-immunoprecipitation was used to explore the physical interaction of SERCA3b with Bcl-2Δ21. In a control experiment, microsomes alone were incubated at 37°C for 1 hr and subsequently 1 μg of the anti-Bcl-2 antibody was added, and the mixture was incubated at 4°C for 2 hrs. We observed that small levels of SERCA3b co-immunoprecipitated, likely via interaction with endogenous Bcl-2 present in the microsomes (Figure 4A, lane 1). To a separate sample of microsomes, we added Bcl-2Δ21 to a molar ratio of SERCA3b:Bcl-2Δ21=1:30. Analysis with the PL/IM430 antibody revealed that significantly higher levels of SERCA3b co-immunoprecipitated when exogenous Bcl-2Δ21 was present in the microsomes (Figure 4A, lane 2). Western blot analysis with the anti-Bcl-2 antibody

was used to detect the amount of endogenous Bcl-2 or added Bcl-2Δ21 associated with SERCA3b (Figure 4B).

Figure 4C shows a comparison of co-immunoprecipitations carried out with two different molar ratios of SERCA3b to Bcl-2Δ21, 1:30 and 1:6, along with various controls. Microsomes isolated from SERCA3b overexpressing cells alone (lane 1) and with Bcl-2Δ21 added to the microsomes (SERCA3b:Bcl-2Δ21=1:30) (lane 2) were incubated at 37°C for 1 hr followed by immunoprecipitation with the anti-Bcl-2 antibody. Western blot analysis with PL/IM430 confirms the immunoprecipitation of SERCA3b. Lanes 5 and 6 represent a similar experiment except for the different molar ratio of SERCA3b:Bcl-2Δ21=1:6. Despite a lower amount of Bcl-2Δ21 used in the experiment shown in lane 6 (as compared to lane 2), lane 6 indicates higher yields of SERCA3b co-immunoprecipitation. We have observed a similar behavior during the co-immunoprecipitation of SERCA1 with Bcl-2Δ21 (unpublished results). It is possible that these results may be related to Bcl-2-induced conformational changes of SERCA3b (see below) and SERCA1 [32, 40]. Potentially the unfolded [32, 40] form of SERCA has a different affinity to Bcl-2 resulting in a less efficient co-immunoprecipitation. A lower ratio of Bcl-2Δ21 to SERCA3b results in a less efficient unfolding, and, consequently more efficient co-immunoprecipitation. Conversely, it is also possible that a large excess of Bcl-2Δ21 will promote Bcl-2Δ21 dimerization, which may lower the amount of Bcl-2Δ21 available for co-immunoprecipitation. Microsomes isolated from HEK-293 cells not overexpressing SERCA3b incubated without (lane 3) and with added Bcl-2Δ21 (lane 4), were included as controls. These data clearly indicate that both purified Bcl-2Δ21 and endogenous Bcl-2 can form a stable immunocomplex with SERCA3b in microsomal proteins, and this, once again, confirms the interaction of SERCA3b with Bcl-2.

3.5. Sucrose density fractionation of microsomal proteins and effect of Bcl-2Δ21

We used sucrose density fractionation of microsomes to evaluate whether Bcl-2Δ21 displaces SERCA3b from membrane domains, which we referred to as caveolae-related domains [40]. When microsomes alone were fractionated, SERCA3b was confined to the low-density sucrose fraction (Figure 5B). To study the effect of Bcl-2Δ21 on the distribution of SERCA3b, purified Bcl-2Δ21 was added to microsomes at a molar ratio of SERCA3b:Bcl-2Δ21=1:28. We observed that the addition of Bcl-2Δ21 resulted in a partial shift of SERCA3b to higher-density fractions (Figure 5A, lanes 6–9). These data are consistent with our earlier *in vitro* experiment with SERCA1 [40]. Higher molecular weight bands (>100k Da) in Figure 5 represent SERCA3b aggregates. The differential aggregation of SERCA3b in the presence and absence of Bcl-2Δ21 may depend on the relative amount of SERCA3b in the fraction.

3.6. SERCA3b interacts with Bcl-2 in cell culture

In the following, we will provide evidence for the inactivation of Bcl-2 with SERCA3b in cell culture. For this, Bcl-2 was transiently expressed in SERCA3b-overexpressing cells. SERCA activity was measured in both preparations and the activities were normalized to the amount of SERCA3b present in the preparations. Figure 6A presents the data collected from five replicates of the same microsome preparation, which clearly show that co-expression of

Bcl-2 in SERCA3b-overexpressing cells leads to a reduction of SERCA activity in microsomes isolated from these cells. The partial inactivation of SERCA3b by Bcl-2 overexpression was observed in at least eight independent experiments (see Figure S2 in the Supplementary Information). The percentage inhibition of SERCA3b activity ranged between 19% and 62%, probably due to the variation in Bcl-2 expression levels as a result of transient transfection. Figure 6B shows the average Ca^{2+}-ATPase activity in SE3/Vec and SE3/Bcl-2 of eight different microsome preparations. There was no significant change in the expression level of SERCA3b as a result of Bcl-2 expression in comparison to only SERCA3b-overexpresing cells, but a significantly higher Bcl-2 expression level was detected using transient transfection with the Bcl-2 vector.

In both SERCA3b and Bcl-2 overexpressing cells, there was a higher molecular weight band very close to the Bcl-2 band and both were recognized by the Bcl-2 antibody (Figure S4). This may represent the phosphorylated form of Bcl-2. We, therefore, analyzed microsomes isolated from SE3/Vec and SE3/Bcl-2 using Thr56- and Ser70-phosphorylation sequence-specific antibodies. We observed that Thr56 was phosphorylated in microsomes from both SERCA3b- and Bcl-2-overexpressing microsomes (SE3/Bcl-2). It is reported that Bcl-2 phosphorylation stimulates its anti-apoptotic functions [41, 42].

It has been reported that G145 is a highly conserved residue in the Bcl-2 protein family, and that G145E mutation abolishes the anti-apoptotic functions of Bcl-2 [43, 44]. If Bcl-2-dependent SERCA inactivation is significant for apoptosis, we would expect that the G145E-Bcl-2 mutant should not inactivate SERCA3b. To assess the effect of G145E-Bcl-2 on SERCA3b, we measured the SERCA activity in microsomes isolated from SERCA3b-overexpressing HEK-293 cells (SE3), SERCA3b overexpressing cells transfected with empty vector (SE3/Vec), SERCA3b overexpressing cells transfected with Bcl-2 DNA (SE3/Bcl-2), and SERCA3b overexpressing cells transfected with G145E-Bcl-2 DNA (SE3/G145E) (Figure 7). A similar experiment was carried out as explained in 2.3 except serum was introduced into the cell culture media immediately after the transfection (Figure S3). The ATPase activities were normalized to the amount of SERCA3b. The expression levels of SERCA3b, Bcl-2 and G145E were analyzed using Western blotting, and significantly higher levels of both Bcl-2 and G145E proteins were observed by transient transfection when compared to the level of endogenous Bcl-2 in SERCA3b-overexpressing cells. The activity difference between SE3/Bcl-2 and SE3/G145E represents the effect of Bcl-2 on the activity of SERCA3b. There is a significant difference for SERCA3b inactivation between SE3/Bcl-2 and SE3/G145E, which parallels the anti-apoptotic function of Bcl-2[43, 44].

3.7. FITC labeling of SERCA in microsomes from HEK-293 cells overexpressing SERCA3b and Bcl-2

FITC specifically reacts with Lys515 on SERCA, and the reaction with FITC is a measure of the structural integrity of the nucleotide-binding domain (N-domain) of SERCA [45]. FITC reaction with SERCA3b was analyzed using microsomes isolated from SERCA3b-overexpressing cells transfected with either empty vector or Bcl-2 encoding vector. Figure 8 indicates that the reaction of FITC with SERCA was significantly reduced in cells, which overexpress both SERCA3b and Bcl-2 compared to cells, which overexpress only

SERCA3b. The decrease in FITC labeling of SERCA is consistent with a change of structural integrity of the N-domain, and likely the overall conformation of SERCA. These results are consistent with our *in vitro* experiment, in which we observed Bcl-2Δ21-dependent loss of SERCA1 FITC labeling [33]. Under our experimental conditions, FITC predominantly labeled SERCA3b; however, labeling of other proteins was also visible when the blot was exposed for longer time periods.

3.8. Co-immunoprecipitation of SERCA3b and Bcl-2 from microsomes of HEK-293 cells overexpressing both SERCA3b and Bcl-2

Microsomes isolated from HEK-293 cells overexpressing SERCA3b alone co-immunoprecipitated less SERCA3b with Bcl-2 than HEK-293 cells overexpressing both SERCA3b and Bcl-2 (Figure 9, lanes 1 and 2). The data displayed in Figure 4C show that a higher Bcl-2:SERCA3b ratio resulted in less co-immunoprecipitation of both proteins (lanes 2 and 6). This is rationalized by Bcl-2-dependent structural changes which results in SERCA3b less available for co-immunoprecipitation. *In vitro*, we have shown that prolonged incubation of SERCA1a with Bcl-2Δ21 resulted in a decrease of co-immunoprecipitation (unpublished results). For example, while a 15 min incubation of SERCA1a in SR membranes with Bcl-2Δ21 resulted in efficient co-immunoprecipitation, extending the incubation time to >45 min resulted in a significant decrease of the yields of co-immunoprecipitated SERCA1a (unpublished results).

4. Discussion

Elevated Bcl-2 expression in cancer cells is well known [46]. An increasing number of publications show significant roles of SERCA3 isoforms in various pathologies and physiologic processes. For example, diminished expression and mutations of SERCA3 have been reported for cancer, such as colon and gastric cancer [47, 48]. SERCA3 may be required for nitric oxide synthase activity in platelets, compromised by hypertension [49]. Knockout of SERCA3 significantly impairs endothelium-dependent relaxation of vascular smooth muscle [50], likely associated with impaired activation of nitric oxide synthase. SERCA3 levels are induced during differentiation of various cell types, and in cancer cells SERCA3 displays a complex pattern of up- and downregulation during cell differentiation and at various stages of cancer [51]. This pattern of up- and downregulation is sufficiently distinct that SERCA3 expression has been suggested as a tumor marker to evaluate the progression of cancer [52]. An important distinction can be made between SERCA2- and SERCA3-associated storage of calcium [51, 53]. For example, in control HL-60 cells SERCA-dependent calcium uptake proceeds ca. 68% via SERCA2b, into a SERCA2-associated compartment, and 32% via SERCA3 into a SERCA3-associated compartment. In contrast, differentiated HL-60 cells display the opposite behavior, where ca. 60% of calcium is taken up via SERCA3 into a SERCA-associated pool, and 40% via SERCA2b into a SERCA2-associated pool. Noteworthy, SERCA3 has a significantly lower calcium affinity compared to SERCA2, indicating major differences in calcium transport between control and differentiated HL-60 cells.

Our investigation of Bcl-2 and SERCA3 interaction may provide important additional information on the mechanisms of Bcl-2 action. Evidence for the interaction of Bcl-2 with SERCA was first documented by Kuo et al. using co-immunoprecipitation studies of Bcl-2 with SERCA1a [30]. Subsequently, Dremina et al. published evidence for a direct *in vitro* interaction of Bcl-2 with SERCA1a using SR fractions and both purified Bcl-2Δ21 and Bcl-2 [32].

Our data show that Bcl-2 interacts with and partially inhibits SERCA3b *in vitro* and in cell culture. A partial inactivation of SERCA is biologically more meaningful while a complete inhibition might cause ER Ca^{2+} levels to drop too much, followed by UPR-induced apoptosis due to ER stress. FITC is considered as a marker of the structural integrity of the N-domain of SERCA. FITC specifically labels Lys515 of SERCA, which is located close to the nucleotide binding site of the N-domain [35, 45]. Our FITC labeling data suggest that the N-domain of SERCA3b may be involved in the mechanism of Bcl-2/SERCA3b interaction. Therefore, partial inactivation of SERCA3b by Bcl-2 may be a consequence of a physical change in the N-domain. Any structural damage to the N-domain could influence its mobility and cause SERCA inactivation; interestingly, it was reported that the pre-incubation of SERCA with ATP prior to the reaction with hydroxyl radicals protected SERCA from hydroxyl radical-induced inactivation [54]. It is, however, also possible that the overall conformation of SERCA3b is altered by the Bcl-2 interaction, and, as a result, FITC labeling capacity of SERCA3b is decreased.

The concept of a Bcl-2-induced SERCA3b conformational transition would be consistent with our co-immunoprecipitation data. Here, less efficient co-immunoprecipitation was detected in the cells which contained high levels of Bcl-2. High Bcl-2 levels would cause unfolding of SERCA3b, which could lead to less efficient co-immunoprecipitation, potentially due to a different affinity of unfolded SERCA3b to Bcl-2. However, we note that higher levels of Bcl-2 also increase the potential for Bcl-2 dimerization (or interaction with other Bcl-2 family proteins), potentially decreasing the amount of Bcl-2 monomers available for interaction with SERCA.

Bcl-2 expression levels and cell viability are closely correlated. Although the overexpression of Bcl-2 would be expected to promote cell survival, loss of cell viability has also been reported [55, 56], and it was speculated that high Bcl-2 levels endorse Ca^{2+}- and ROS-dependent apoptosis. On the other hand, moderate levels of Bcl-2 expression always preserve normal cell viability and high levels of Bcl-2 lead to abnormal cell loss [57]. We observed in our experiments that a fraction of HEK-293 cells encoding SERCA3b lost viability after additional Bcl-2 transfection. This observation might be rationalized by an ER-stress-induced cell death due to SERCA inactivation.

SERCAs are regulated by two low molecular weight proteins, phospholamban (PLB) and sarcolipin (SLN) [58]. PLB is expressed at higher levels in the heart where it regulates SERCA2 by changing the pump's affinity for Ca^{2+} depending on the phosphorylation state of PLB [59]. The co-expression of SLN with SERCA1a or SERCA2a in HEK cells decreased the apparent Ca^{2+} affinity of the SERCA pump, suggesting that SLN acts as an inhibitor. When SLN was co-expressed with PLB, a super-inhibitory effect was observed

[60]. In addition to SLN and PLB, there are a few other proteins reported to interact with SERCA2: sarcalumenin [61], histidine rich Ca^{2+}-binding protein [62], Bcl-2 [63], calreticulin and calnexin [64].

The SERCA family consists of three major isoforms, SERCA1, SERCA2 and SERCA3, where SERCA3 displays unique characteristics, such as a reduced apparent affinity for Ca^{2+}. The physiological relevance of such functional differences between different SERCA isoforms is yet to be evaluated. It may be possible that different isoforms function at different Ca^{2+} concentrations and, therefore, SERCA3 might be involved in Ca^{2+} transport under at Ca^{2+} concentrations. It is also important to note that members of the SERCA family share a high degree of similarities in their basic structure. Nevertheless, a slight variation in the sequence causes different susceptibilities towards H_2O_2-induced inactivation where SERCA2b is inactivated more efficiently than SERCA3 [65].

In summary, Bcl-2 interacts with and inhibits the SERCA3b isoform both *in vitro* and in cell culture, and SERCA3b inactivation is accompanied with a Bcl-2-dependent conformational change of SERCA3b.

Supplementary Material

Refer to Web version on PubMed Central for supplementary material.

Acknowledgments

We gratefully acknowledge the generous gift of HEK-293 cells, which were stably transfected with a human SERCA3b-encoding vector from Dr. Jocelyne Enouf (INSERM, Villejuif, France), and financial support from the NIH (PO1AG12993).

Abbreviations

SERCA	sarco/endoplasmic reticulum Ca^{2+}-ATPase
Bcl-2	B-cell lymphoma 2
Bcl-2Δ21	human recombinant Bcl-2 with the 21 C-terminal amino acids deleted
ER	endoplasmic reticulum
GST	glutathione S-transferase
DMEM	Dulbecco’s modified Eagle’s medium
ATP2A3	partial recombinant protein of SERCA3 with a GST tag at N-terminal
FITC	fluorescein isothiocyanate

References

1. Renehan AG, Booth C, Potten CS. What is apoptosis, and why is it important? Br Med J. 2001; 322:1536–1538. [PubMed: 11420279]
2. Giorgi C, Romagnoli A, Pinton P, Rizzuto R. Ca^{2+} signaling, mitochondria and cell death. Curr Mol Med. 2008; 8:119–130. [PubMed: 18336292]

3. Monteith GR, McAndrew D, Faddy HM, Roberts-Thomson SJ. Calcium and cancer: targeting Ca^{2+} transport. Nat Rev Cancer. 2007; 7:519–530. [PubMed: 17585332]
4. Berridge MJ, Bootman MD, Roderick HL. Calcium signalling: dynamics, homeostasis and remodelling. Nat Rev Mol Cell Biol. 2003; 4:517–529. [PubMed: 12838335]
5. Demaurex N, Distelhorst C. Cell biology. Apoptosis--the calcium connection. Science. 2003; 300:65–67. [PubMed: 12677047]
6. Oakes SA, Opferman JT, Pozzan T, Korsmeyer SJ, Scorrano L. Regulation of endoplasmic reticulum Ca^{2+} dynamics by proapoptotic Bcl-2 family members. Biochem Pharmacol. 2003; 66:1335–1340. [PubMed: 14555206]
7. Lam AK, Galione A. The endoplasmic reticulum and junctional membrane communication during calcium signaling. Biochim Biophys Acta. 2013; 1833:2542–2559. [PubMed: 23770047]
8. Lytton J, Westlin M, Burk SE, Shull GE, MacLennan DH. Functional comparisons between isoforms of the sarcoplasmic or endoplasmic reticulum family of calcium pumps. J Biol Chem. 1992; 267:14483–14489. [PubMed: 1385815]
9. Dode L, Vilsen B, Van Baelen K, Wuytack F, Clausen JD, Andersen JP. Dissection of the functional differences between sarco(endo)plasmic reticulum Ca^{2+}-ATPase (SERCA) 1 and 3 isoforms by steady-state and transient kinetic analyses. J Biol Chem. 2002; 277:45579–45591. [PubMed: 12207029]
10. Wuytack F, Dode L, Baba-Aissa F, Raeymaekers L. The SERCA3-type of organellar Ca^{2+} pumps. Biosci Rep. 1995; 15:299–306. [PubMed: 8825032]
11. Wuytack F, Papp B, Verboomen H, Raeymaekers L, Dode L, Bobe R, Enouf J, Bokkala S, Authi KS, Casteels R. A sarco/endoplasmic reticulum Ca^{2+}-ATPase 3-type Ca^{2+} pump is expressed in platelets, in lymphoid cells, and in mast cells. J Biol Chem. 1994; 269:1410–1416. [PubMed: 8288608]
12. Anger M, Samuel JL, Marotte F, Wuytack F, Rappaport L, Lompre AM. The sarco(endo)plasmic reticulum Ca^{2+}-ATPase mRNA isoform, SERCA 3, is expressed in endothelial and epithelial cells in various organs. FEBS Lett. 1993; 334:45–48. [PubMed: 8224225]
13. Bobe R, Bredoux R, Corvazier E, Andersen JP, Clausen JD, Dode L, Kovacs T, Enouf J. Identification, expression, function, and localization of a novel (sixth) isoform of the human sarco/endoplasmic reticulum Ca^{2+}-ATPase 3 gene. J Biol Chem. 2004; 279:24297–24306. [PubMed: 15028735]
14. Dally S, Monceau V, Corvazier E, Bredoux R, Raies A, Bobe R, del Monte F, Enouf J. Compartmentalized expression of three novel sarco/endoplasmic reticulum Ca^{2+}-ATPase 3 isoforms including the switch to ER stress, SERCA3f, in non-failing and failing human heart. Cell Calcium. 2009; 45:144–154. [PubMed: 18947868]
15. Gross A, McDonnell JM, Korsmeyer SJ. Bcl-2 family members and the mitochondria in apoptosis. Genes Dev. 1999; 13:1899–1911. [PubMed: 10444588]
16. Walensky LD. Bcl-2 in the crosshairs: tipping the balance of life and death. Cell Death Differ. 2006; 13:1339–1350. [PubMed: 16763614]
17. Thomenius MJ, Distelhorst CW. Bcl-2 on the endoplasmic reticulum: protecting the mitochondria from a distance. J Cell Sci. 2003; 116:4493–4499. [PubMed: 14576343]
18. He H, Lam M, McCormick TS, Distelhorst CW. Maintenance of calcium homeostasis in the endoplasmic reticulum by Bcl-2. J Cell Biol. 1997; 138:1219–1228. [PubMed: 9298978]
19. Shimizu S, Narita M, Tsujimoto Y. Bcl-2 family proteins regulate the release of apoptogenic cytochrome c by the mitochondrial channel VDAC. Nature. 1999; 399:483–487. [PubMed: 10365962]
20. Tsujimoto Y, Shimizu S. The voltage-dependent anion channel: an essential player in apoptosis. Biochimie. 2002; 84:187–193. [PubMed: 12022949]
21. Harris MH, Thompson CB. The role of the Bcl-2 family in the regulation of outer mitochondrial membrane permeability. Cell Death Differ. 2000; 7:1182–1191. [PubMed: 11175255]
22. Pinton P, Ferrari D, Magalhaes P, Schulze-Osthoff K, Di Virgilio F, Pozzan T, Rizzuto R. Reduced loading of intracellular Ca^{2+} stores and downregulation of capacitative Ca^{2+} influx in Bcl-2-overexpressing cells. J Cell Biol. 2000; 148:857–862. [PubMed: 10704437]

23. Vanden Abeele F, Skryma R, Shuba Y, Van Coppenolle F, Slomianny C, Roudbaraki M, Mauroy B, Wuytack F, Prevarskaya N. Bcl-2-dependent modulation of Ca^{2+} homeostasis and store-operated channels in prostate cancer cells. Cancer Cell. 2002; 1:169–179. [PubMed: 12086875]
24. Foyouzi-Youssefi R, Arnaudeau S, Borner C, Kelley WL, Tschopp J, Lew DP, Demaurex N, Krause KH. Bcl-2 decreases the free Ca^{2+} concentration within the endoplasmic reticulum. Proc Natl Acad Sci USA. 2000; 97:5723–5728. [PubMed: 10823933]
25. Palmer AE, Jin C, Reed JC, Tsien RY. Bcl-2-mediated alterations in endoplasmic reticulum Ca^{2+} analyzed with an improved genetically encoded fluorescent sensor. Proc Natl Acad Sci USA. 2004; 101:17404–17409. [PubMed: 15585581]
26. Chen R, Valencia I, Zhong F, McColl KS, Roderick HL, Bootman MD, Berridge MJ, Conway SJ, Holmes AB, Mignery GA, Velez P, Distelhorst CW. Bcl-2 functionally interacts with inositol 1,4,5-trisphosphate receptors to regulate calcium release from the ER in response to inositol 1,4,5-trisphosphate. J Cell Biol. 2004; 166:193–203. [PubMed: 15263017]
27. Rong YP, Aromolaran AS, Bultynck G, Zhong F, Li X, McColl K, Matsuyama S, Herlitze S, Roderick HL, Bootman MD, Mignery GA, Parys JB, De Smedt H, Distelhorst CW. Targeting Bcl-2-IP3 receptor interaction to reverse Bcl-2's inhibition of apoptotic calcium signals. Mol Cell. 2008; 31:255–265. [PubMed: 18657507]
28. Rong YP, Bultynck G, Aromolaran AS, Zhong F, Parys JB, De Smedt H, Mignery GA, Roderick HL, Bootman MD, Distelhorst CW. The BH4 domain of Bcl-2 inhibits ER calcium release and apoptosis by binding the regulatory and coupling domain of the IP3 receptor. Proc Natl Acad Sci USA. 2009; 106:14397–14402. [PubMed: 19706527]
29. Zhong F, Davis MC, McColl KS, Distelhorst CW. Bcl-2 differentially regulates Ca^{2+} signals according to the strength of T cell receptor activation. J Cell Biol. 2006; 172:127–137. [PubMed: 16391001]
30. Xu L, Kong D, Zhu L, Zhu W, Andrews DW, Kuo TH. Suppression of IP3-mediated calcium release and apoptosis by Bcl-2 involves the participation of protein phosphatase 1. Mol Cell Biochem. 2007; 295:153–165. [PubMed: 16874461]
31. Harr MW, Distelhorst CW. Apoptosis and autophagy: decoding calcium signals that mediate life or death. Cold Spring Harb Perspect Biol. 2010; 2:a005579. [PubMed: 20826549]
32. Dremina ES, Sharov VS, Kumar K, Zaidi A, Michaelis EK, Schöneich C. Anti-apoptotic protein Bcl-2 interacts with and destabilizes the sarcoplasmic/endoplasmic reticulum Ca^{2+}-ATPase (SERCA). Biochem J. 2004; 383:361–370. [PubMed: 15245329]
33. Dremina ES, Sharov VS, Schöneich C. Heat-shock proteins attenuate SERCA inactivation by the anti-apoptotic protein Bcl-2: possible implications for the ER Ca^{2+}-mediated apoptosis. Biochem J. 2012; 444:127–139. [PubMed: 22360692]
34. Maruyama K, MacLennan DH. Mutation of aspartic acid-351, lysine-352, and lysine-515 alters the Ca^{2+} transport activity of the Ca^{2+}-ATPase expressed in COS-1 cells. Proc Natl Acad Sci USA. 1988; 85:3314–3318. [PubMed: 2966962]
35. Tupling AR, Gramolini AO, Duhamel TA, Kondo H, Asahi M, Tsuchiya SC, Borrelli MJ, Lepock JR, Otsu K, Hori M, MacLennan DH, Green HJ. HSP70 binds to the fast-twitch skeletal muscle sarco(endo)plasmic reticulum Ca^{2+}-ATPase (SERCA1a) and prevents thermal inactivation. J Biol chem. 2004; 279:52382–52389. [PubMed: 15371420]
36. Chandrasekera PC, Kargacin ME, Deans JP, Lytton J. Determination of apparent calcium affinity for endogenously expressed human sarco(endo)plasmic reticulum calcium-ATPase isoform SERCA3. Am J Physiol Cell Physiol. 2009; 296:C1105–C1114. [PubMed: 19225163]
37. Blanchard-Fillion B, Souza JM, Friel T, Jiang GC, Vrana K, Sharov V, Barron L, Schoneich C, Quijano C, Alvarez B, Radi R, Przedborski S, Fernando GS, Horwitz J, Ischiropoulos H. Nitration and inactivation of tyrosine hydroxylase by peroxynitrite. J Biol Chem. 2001; 276:46017–46023. [PubMed: 11590168]
38. Bobe R, Bredoux R, Corvazier E, Lacabaratz-Porret C, Martin V, Kovacs T, Enouf J. How many Ca^{2+}-ATPase isoforms are expressed in a cell type? A growing family of membrane proteins illustrated by studies in platelets. Platelets. 2005; 16:133–150. [PubMed: 16011958]

39. Poch E, Leach S, Snape S, Cacic T, MacLennan DH, Lytton J. Functional characterization of alternatively spliced human SERCA3 transcripts. Am J Physiol. 1998; 275:C1449–C1458. [PubMed: 9843705]
40. Dremina ES, Sharov VS, Schöneich C. Displacement of SERCA from SR lipid caveolaerelated domains by Bcl-2: a possible mechanism for SERCA inactivation. Biochemistry. 2006; 45:175–184. [PubMed: 16388593]
41. Deng X, Gao F, Flagg T, May WS Jr. Mono- and multisite phosphorylation enhances Bcl2's antiapoptotic function and inhibition of cell cycle entry functions. Proc Natl Acad Sci USA. 2004; 101:153–158. [PubMed: 14660795]
42. Ito T, Deng X, Carr B, May WS. Bcl-2 phosphorylation required for anti-apoptosis function. J Biol Chem. 1997; 272:11671–11673. [PubMed: 9115213]
43. Gurudutta GU, Verma YK, Singh VK, Gupta P, Raj HG, Sharma RK, Chandra R. Structural conservation of residues in BH1 and BH2 domains of Bcl-2 family proteins. FEBS Lett. 2005; 579:3503–3507. [PubMed: 15949801]
44. Yin XM, Oltvai ZN, Korsmeyer SJ. BH1 and BH2 domains of Bcl-2 are required for inhibition of apoptosis and heterodimerization with Bax. Nature. 1994; 369:321–323. [PubMed: 8183370]
45. Autry JM, Rubin JE, Svensson B, Li J, Thomas DD. Nucleotide activation of the Ca^{2+}-ATPase. J Biol Chem. 2012; 287:39070–39082. [PubMed: 22977248]
46. Fahy BN, Schlieman MG, Mortenson MM, Virudachalam S, Bold RJ. Targeting BCL-2 overexpression in various human malignancies through NF-kappaB inhibition by the proteasome inhibitor bortezomib. Cancer Chemother Pharmacol. 2005; 56:46–54. [PubMed: 15791457]
47. Arbabian A, Brouland JP, Apati A, Paszty K, Hegedus L, Enyedi A, Chomienne C, Papp B. Modulation of endoplasmic reticulum calcium pump expression during lung cancer cell differentiation. FEBS J. 2013; 280:5408–5418. [PubMed: 23157274]
48. Brouland JP, Gelebart P, Kovacs T, Enouf J, Grossmann J, Papp B. The loss of sarco/endoplasmic reticulum calcium transport ATPase 3 expression is an early event during the multistep process of colon carcinogenesis. Am J Pathol. 2005; 167:233–242. [PubMed: 15972967]
49. Martin V, Bredoux R, Corvazier E, Papp B, Enouf J. Platelet Ca^{2+}-ATPases : a plural, species-specific, and multiple hypertension-regulated expression system. Hypertension. 2000; 35:91–102. [PubMed: 10642281]
50. Liu LH, Paul RJ, Sutliff RL, Miller ML, Lorenz JN, Pun RY, Duffy JJ, Doetschman T, Kimura Y, MacLennan DH, Hoying JB, Shull GE. Defective endothelium-dependent relaxation of vascular smooth muscle and endothelial cell Ca^{2+} signaling in mice lacking sarco(endo)plasmic reticulum Ca^{2+}-ATPase isoform 3. J Biol Chem. 1997; 272:30538–30545. [PubMed: 9374548]
51. Papp B, Brouland JP, Arbabian A, Gelebart P, Kovacs T, Bobe R, Enouf J, Varin-Blank N, Apati A. Endoplasmic reticulum calcium pumps and cancer cell differentiation. Biomolecules. 2012; 2:165–186. [PubMed: 24970132]
52. Flores-Peredo L, Rodriguez G, Zarain-Herzberg A. Induction of Cell Differentiation Activates Transcription of the Sarco/Endoplasmic Reticulum Calcium-ATPase 3 Gene (ATP2A3) in Gastric and Colon Cancer Cells. Mol. Carcinogen. 2016; 9999:1–16.
53. Launay S, Gianni M, Kovacs T, Bredoux R, Bruel A, Gelebart P, Zassadowski F, Chomienne C, Enouf J, Papp B. Lineage-specific modulation of calcium pump expression during myeloid differentiation. Blood. 1999; 93:4395–4405. [PubMed: 10361138]
54. Xu KY, Zweier JL, Becker LC. Hydroxyl radical inhibits sarcoplasmic reticulum $Ca2^{+}$-ATPase function by direct attack on the ATP binding site. Circ Res. 1997; 80:76–81. [PubMed: 8978325]
55. Uhlmann EJ, Subramanian T, Vater CA, Lutz R, Chinnadurai G. A potent cell death activity associated with transient high level expression of Bcl-2. J Biol Chem. 1998; 273:17926–17932. [PubMed: 9651399]
56. Wang NS, Unkila MT, Reineks EZ, Distelhorst CW. Transient expression of wild-type or mitochondrially targeted Bcl-2 induces apoptosis, whereas transient expression of endoplasmic reticulum-targeted Bcl-2 is protective against Bax-induced cell death. J Biol Chem. 2001; 276:44117–44128. [PubMed: 11546793]

57. Shinoura N, Yoshida Y, Nishimura M, Muramatsu Y, Asai A, Kirino T, Hamada H. Expression level of Bcl-2 determines anti- or proapoptotic function. Cancer Res. 1999; 59:4119–4128. [PubMed: 10463617]
58. Asahi M, McKenna E, Kurzydlowski K, Tada M, MacLennan DH. Physical interactions between phospholamban and sarco(endo)plasmic reticulum Ca^{2+}-ATPases are dissociated by elevated Ca^{2+}, but not by phospholamban phosphorylation, vanadate, or thapsigargin, and are enhanced by ATP. J Biol Chem. 2000; 275:15034–15038. [PubMed: 10809745]
59. Periasamy M, Bhupathy P, Babu GJ. Regulation of sarcoplasmic reticulum Ca^{2+}-ATPase pump expression and its relevance to cardiac muscle physiology and pathology. Cardiovasc Res. 2008; 77:265–273. [PubMed: 18006443]
60. Morita T, Hussain D, Asahi M, Tsuda T, Kurzydlowski K, Toyoshima C, Maclennan DH. Interaction sites among phospholamban, sarcolipin, and the sarco(endo)plasmic reticulum Ca^{2+}-ATPase. Biochem Biophys Res Commun. 2008; 369:188–194. [PubMed: 18053795]
61. Shimura M, Minamisawa S, Takeshima H, Jiao Q, Bai Y, Umemura S, Ishikawa Y. Sarcalumenin alleviates stress-induced cardiac dysfunction by improving Ca^{2+} handling of the sarcoplasmic reticulum. Cardiovasc Res. 2008; 77:362–370. [PubMed: 18006473]
62. Arvanitis DA, Vafiadaki E, Fan GC, Mitton BA, Gregory KN, Del Monte F, Kontrogianni-Konstantopoulos A, Sanoudou D, Kranias EG. Histidine-rich Ca-binding protein interacts with sarcoplasmic reticulum Ca-ATPase. Am J Physiol Heart Circ Physiol. 2007; 293:H1581–H1589. [PubMed: 17526652]
63. Kuo TH, Kim HR, Zhu L, Yu Y, Lin HM, Tsang W. Modulation of endoplasmic reticulum calcium pump by Bcl-2. Oncogene. 1998; 17:1903–1910. [PubMed: 9788433]
64. Puzianowska-Kuznicka M, Kuznicki J. The ER and ageing II: calcium homeostasis. Ageing Res Rev. 2009; 8:160–172. [PubMed: 19427411]
65. Grover AK, Samson SE, Misquitta CM. Sarco(endo)plasmic reticulum Ca^{2+} pump isoform SERCA3 is more resistant than SERCA2b to peroxide. Am J Physiol. 1997; 273:C420–C425. [PubMed: 9277339]

Highlights

- Bcl-2Δ21 interacts with and partially inhibits SERCA3b isoform.
- Bcl-2 interacts with and partially inhibits SERCA3b in cell culture.
- Both exogenous Bcl-2Δ21 and endogenous Bcl-2 could form a stable immunocomplex with SERCA3b.
- Overexpression of Bcl-2 reduced fluorescein isothiocyanate (FITC) labeling of SERCA3b.

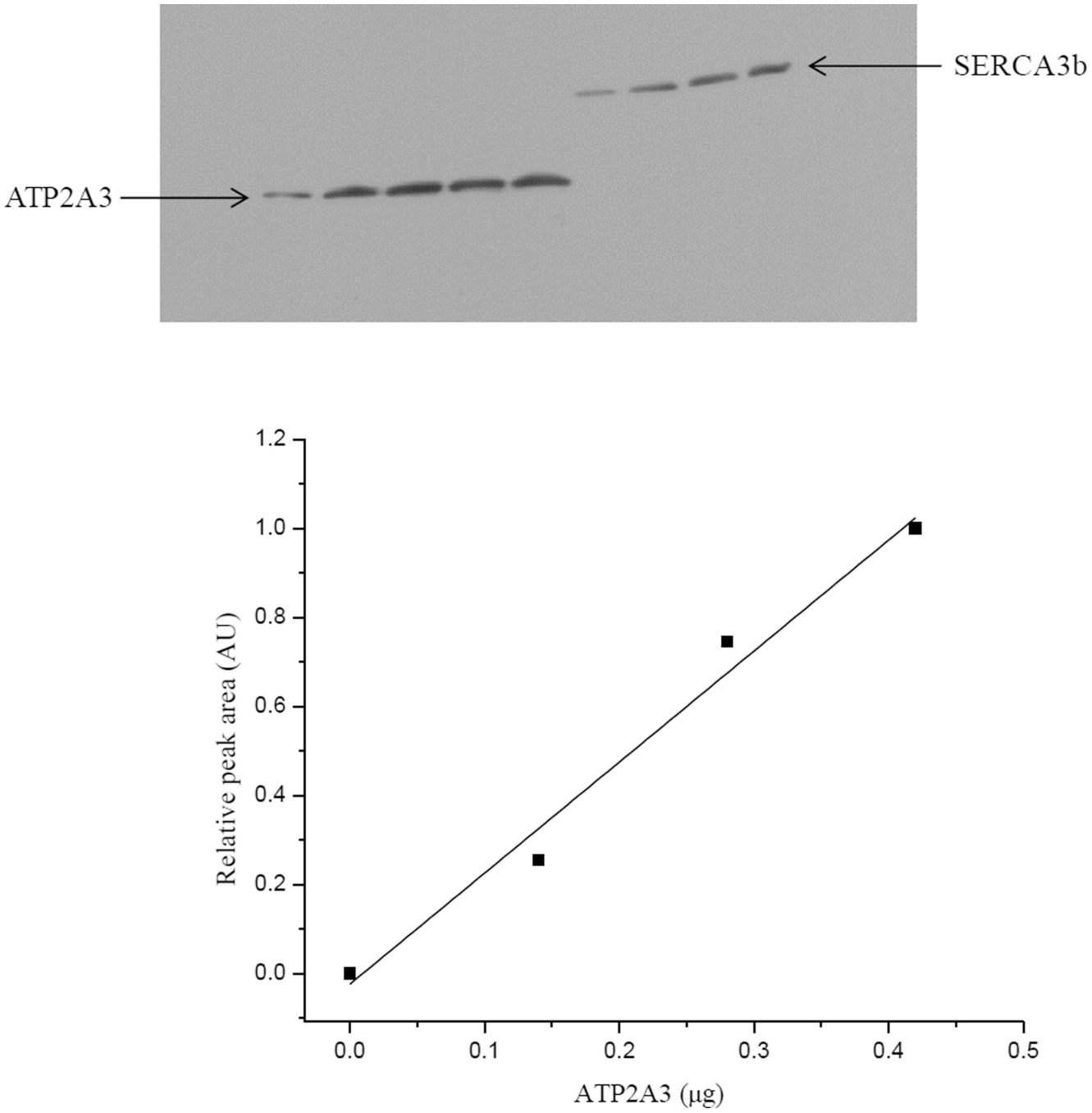

Figure 1. Quantification of SERCA3b in microsomes isolated from SERCA3b overexpressing cells

ATP2A3 and GST were used as described in 2.12.2. First, we quantified recombinant GST and used it as a standard to determine the concentration of ATP2A3. In the final step, we used ATP2A3 as a standard to quantify SERCA3b in microsomal fractions. ***Top:*** 2 μg, 4 μg, 5 μg and 6 μg of microsomal proteins were loaded onto the gel, along with different amounts of ATP2A3, and Western blot analysis was done with the anti-ATP2A3 antibody. ***Bottom:*** A calibration curve was generated by densitometry using relative peak area of ATP2A3 as

explained in 2.12.2 (For ATP2A3 amounts >0.45 μg, we observed signal saturation in the Western blot; these data points were excluded from the calibration).

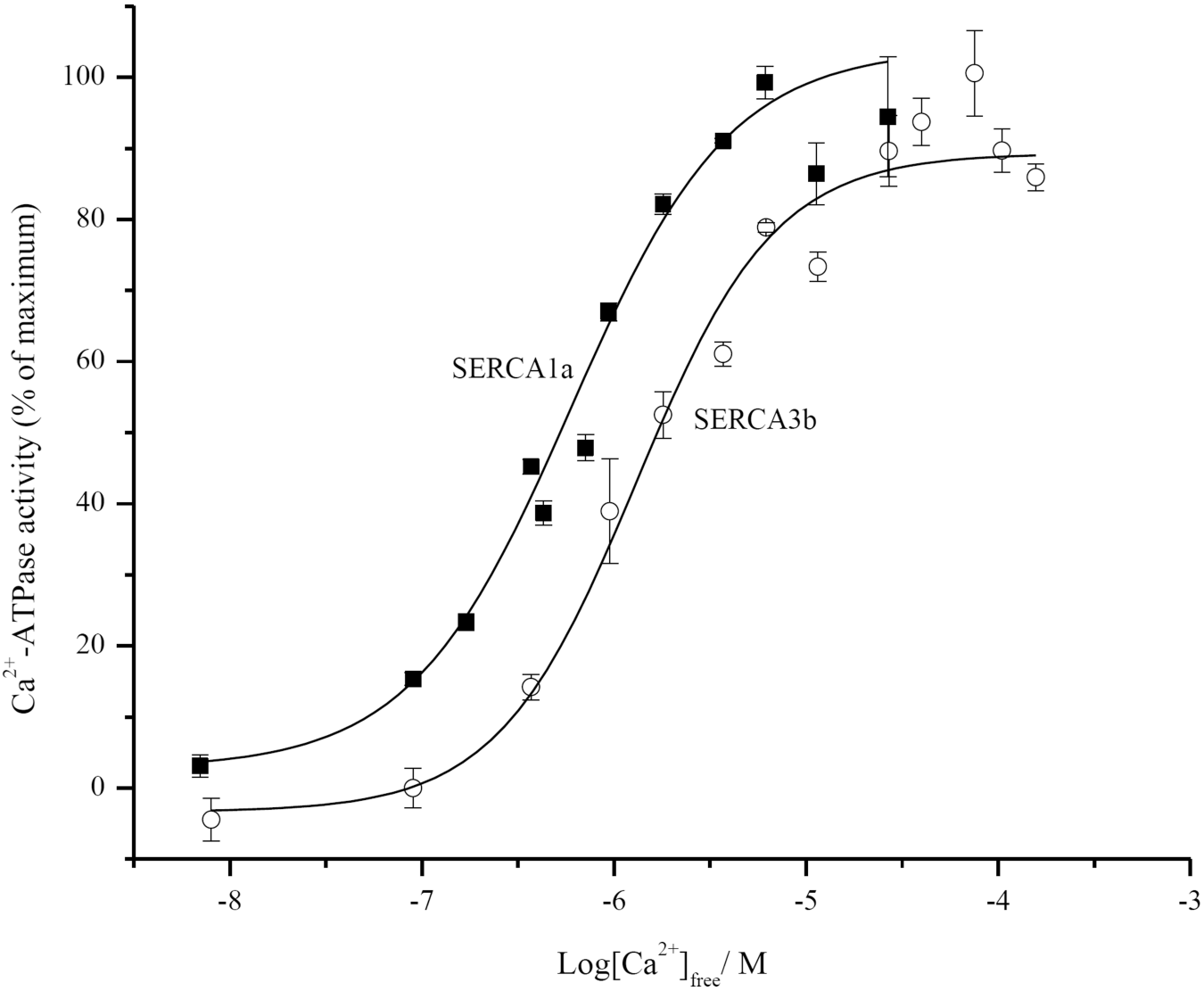

Figure 2. Ca^{2+}-dependent ATPase activity of SERCA3b and SERCA1a at 30°C

Ca^{2+}-ATPase activity of SERCA3b and SERCA1a was determined separately using microsomes isolated from SERCA3b-encoding vector transfected HEK-293 cells and rat skeletal-muscle SR vesicles, respectively.

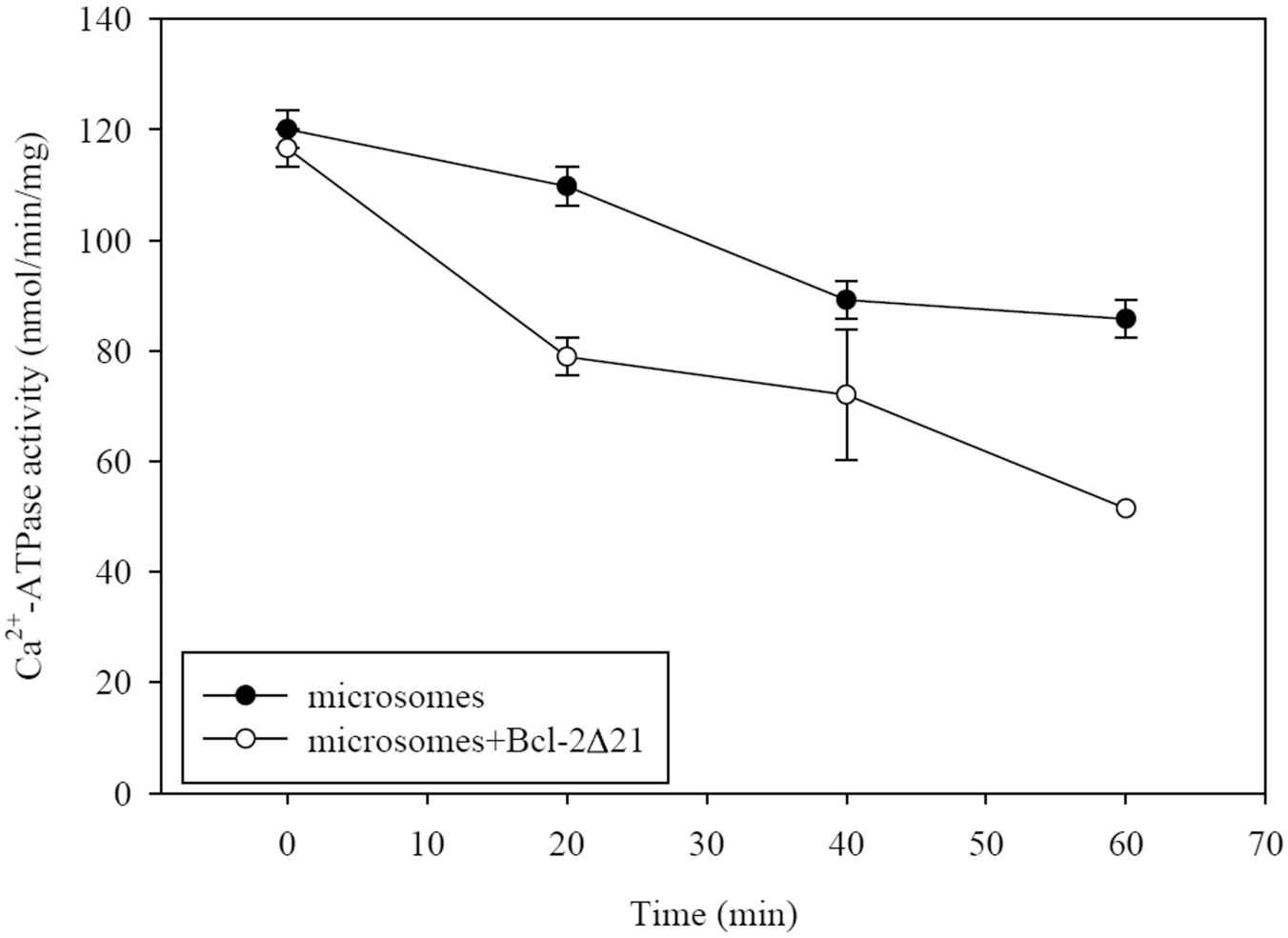

Figure 3. The inhibition of Ca^{2+}-ATPase activity of SERCA3b by Bcl-2Δ21

The Ca^{2+}-ATPase activity of SERCA3b was assayed in the presence and absence of Bcl-2Δ21 at 37°C. Incubation of microsomes isolated from SERCA3b overexpressing cells with Bcl-2Δ21 (molar ratio of SERCA3b:Bcl-2Δ21=3:2) results in a partial inhibition of SERCA3b activity over time. The values shown are the mean±S.E. for three sample replicates; S.E. smaller than symbols are not visible.

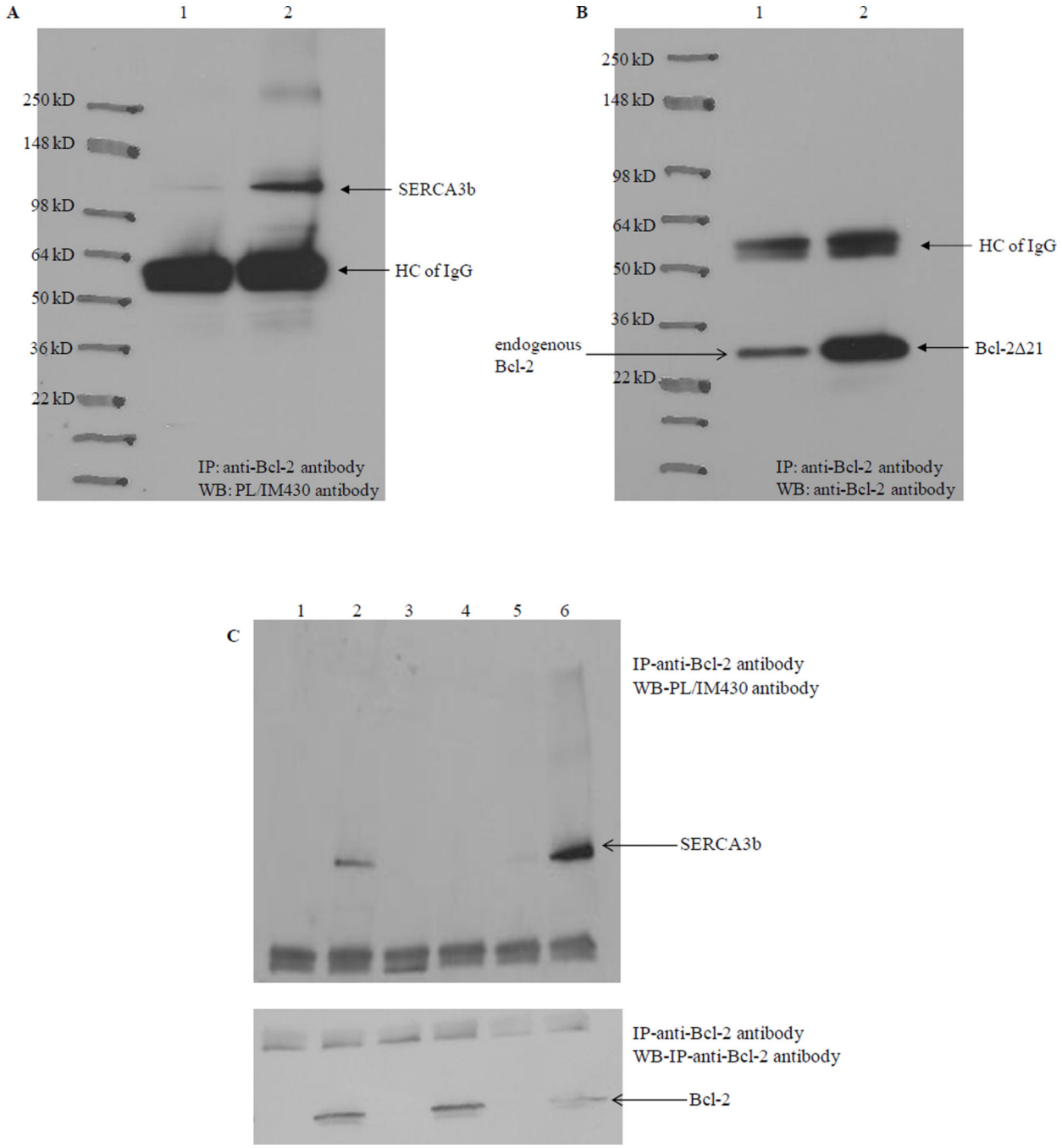

Figure 4. Co-immunoprecipitation of SERCA3b with Bcl-2Δ21 at different SERCA3b:Bcl-2Δ21 molar ratios

(A) Lane 1: microsomes isolated from SERCA3b overexpressing cells without added Bcl-2Δ21; lane 2: microsomes isolated from SERCA3b overexpressing cells with added Bcl-2Δ21; immunoprecipitation with anti-Bcl-2 antibody and analysis with the PL/IM430 antibody. **(B)** The membrane used in Figure 4A was stripped and reprobed with the anti-Bcl-2 antibody. Very intense bands around 55 kDa in both A and B might represent the non-specific binding of antibody heavy chains (HC of IgG). **(C)** Lane 1: microsomes isolated

from SERCA3b-encoding vector transfected cells alone; lane 2: microsomes isolated from SERCA3b-encoding vector transfected cells and Bcl-2Δ21 were incubated at a molar ratio of SERCA3b: Bcl-2Δ21 =1:30 at 37°C; lane 3: microsomes isolated from empty vector (without the sequence for SERCA3b) transfected cells; lane 4: microsomes isolated from empty vector (without the sequence for SERCA3b) transfected cells and added Bcl-2Δ21; lane 5: microsomes isolated from SERCA3b overexpressing cells alone; lane 6: microsomes isolated from SERCA3b overexpressing cells and added Bcl-2Δ21 were incubated at a molar ratio of SERCA3b: Bcl-2Δ21=1:6 at 37°C.

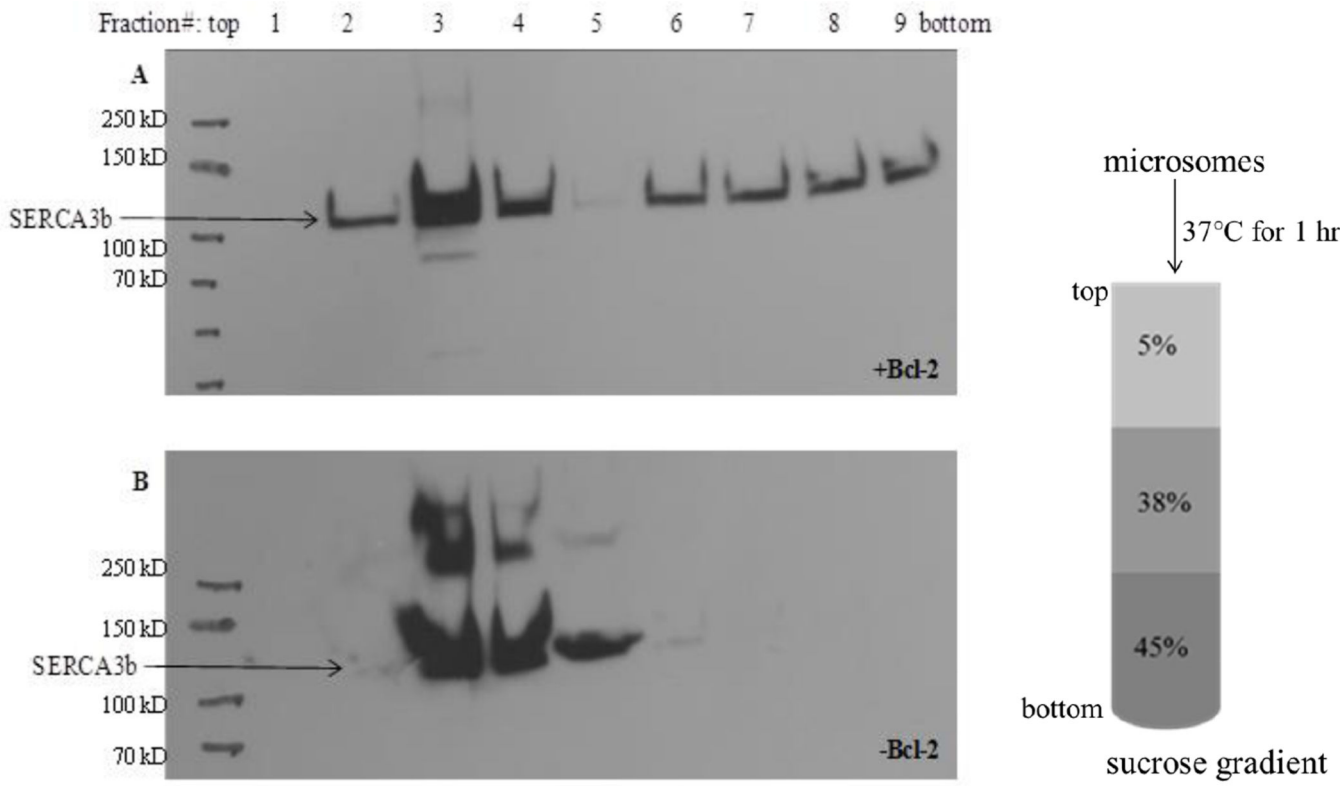

Figure 5. Effect of Bcl-2Δ21 on the distribution of SERCA3b in sucrose-density gradient fractions

Microsomes isolated from SERCA3b-overexpressing HEK-293 cells were incubated with Bcl-2Δ21 (molar ratio of SERCA3b:Bcl-2Δ21 ~1:28) **(A)** and without Bcl-2Δ21 **(B)** at 37°C for 1 hr followed by sucrose density gradient separation. Fractions (1–9) from the sucrose gradient were collected and analyzed by Western blotting with the PL/IM430 antibody. Higher molecular weight bands that are above SERCA3b bands show aggregation of SERCA3b.

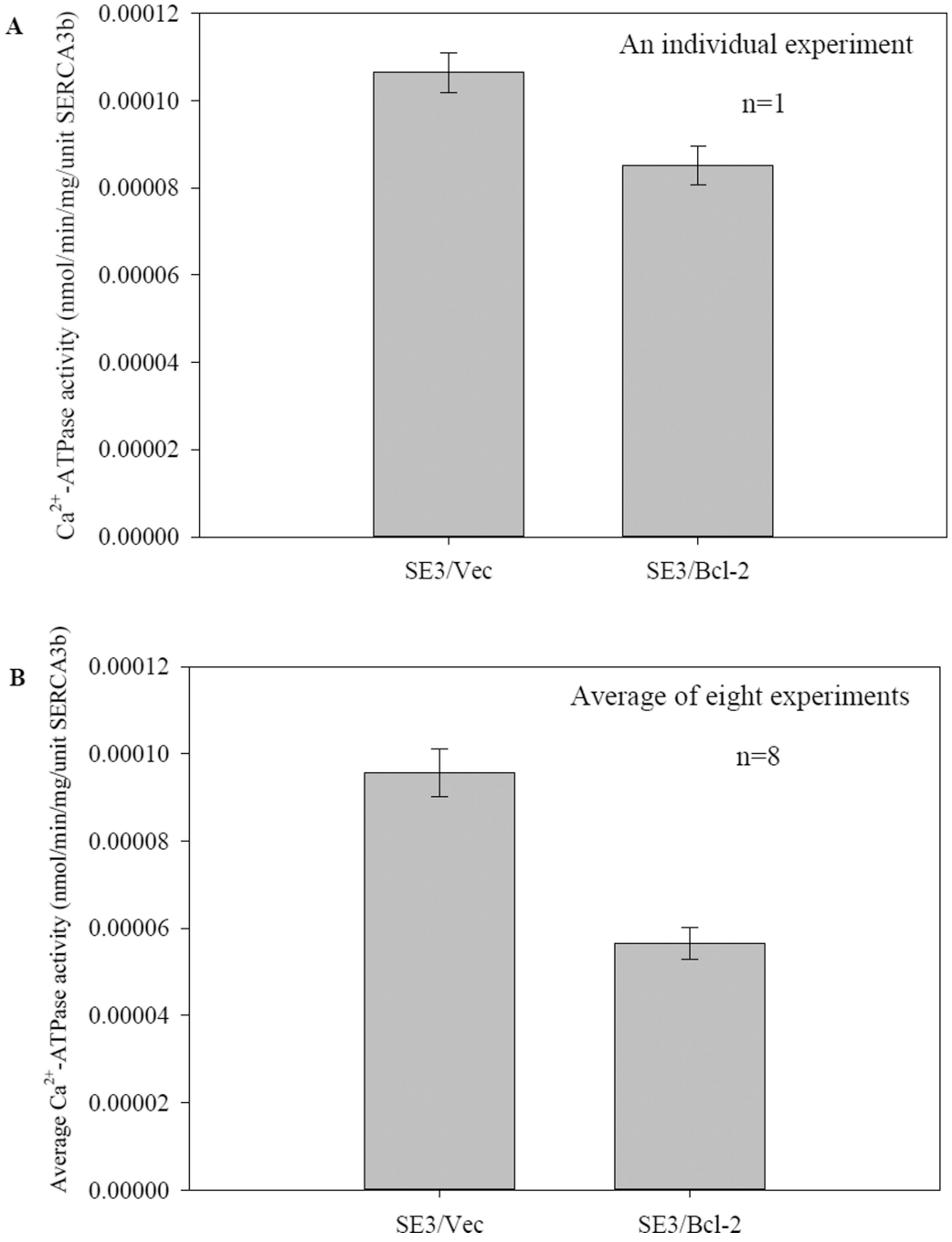

Figure 6. Bcl-2 inhibits Ca^{2+}-ATPase activity of SERCA3b

Ca^{2+}-ATPase activity of SERCA3b was measured using microsomes isolated from HEK-293 cells transfected with a cDNA construct without the sequence for Bcl-2 (SE3/Vec) and microsomes isolated from HEK-293 cells transfected with a Bcl-2-encoding vector (SE3/Bcl-2). Ca^{2+}-ATPase activities were normalized to the SERCA3b content in each sample and levels of SERCA3b and Bcl-2 were revealed by Western blotting with PL/IM430 and anti-Bcl-2 antibody, respectively. Data from an individual experiment are shown in **(A)**. The values shown are the mean±S.E. for five sample replicates; the same trend was observed in

eight different microsome isolations (Figure S2 in the Supplementary Information). Average Ca^{2+}-ATPase activities of eight independent experiments are shown in **(B)**. Ca^{2+}-ATPase activities were normalized per 1 μg of microsomal proteins and then that value was divided by peak area of SERCA3b bands to determine the activity per unit SERCA3b.

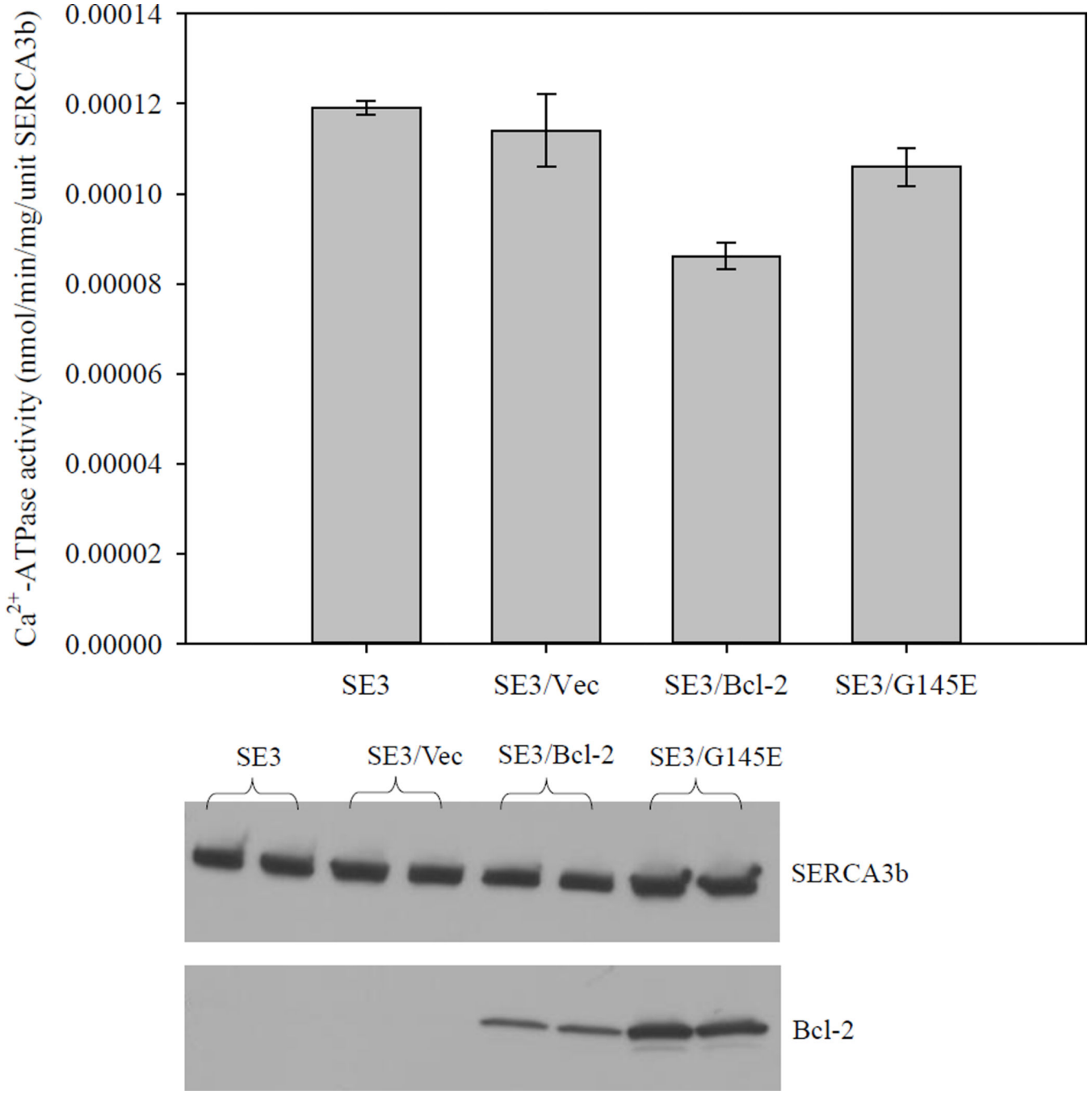

Figure 7. The effect of Bcl-2 and G145E-Bcl-2 expression on Ca^{2+}-ATPase activity of SERCA3b

To test the effect of Bcl-2 and G145E-Bcl-2 expression on the activity of SERCA3b, HEK-293 cells expressing SERCA3b were transfected with a Bcl-2-encoding vector and G145E-Bcl-2-encoding vector, respectively. Experiments were carried out using microsomes isolated from cells expressing SERCA3b (SE3), microsomes isolated from cells transfected with a cDNA construct without the sequence for Bcl-2 (SE3/Vec), microsomes isolated from cells transfected with a Bcl-2-encoding vector (SE3/Bcl-2) and microsomes isolated from cells transfected with a G145E-Bcl-2-encoding vector (SE3/G145E). Levels of SERCA3b

and Bcl-2 were revealed by Western blotting with PL/IM430 and anti-Bcl-2 antibody, respectively. The Ca^{2+}-ATPase activity in each sample was determined using five replicates and mean±S.E. values are shown.

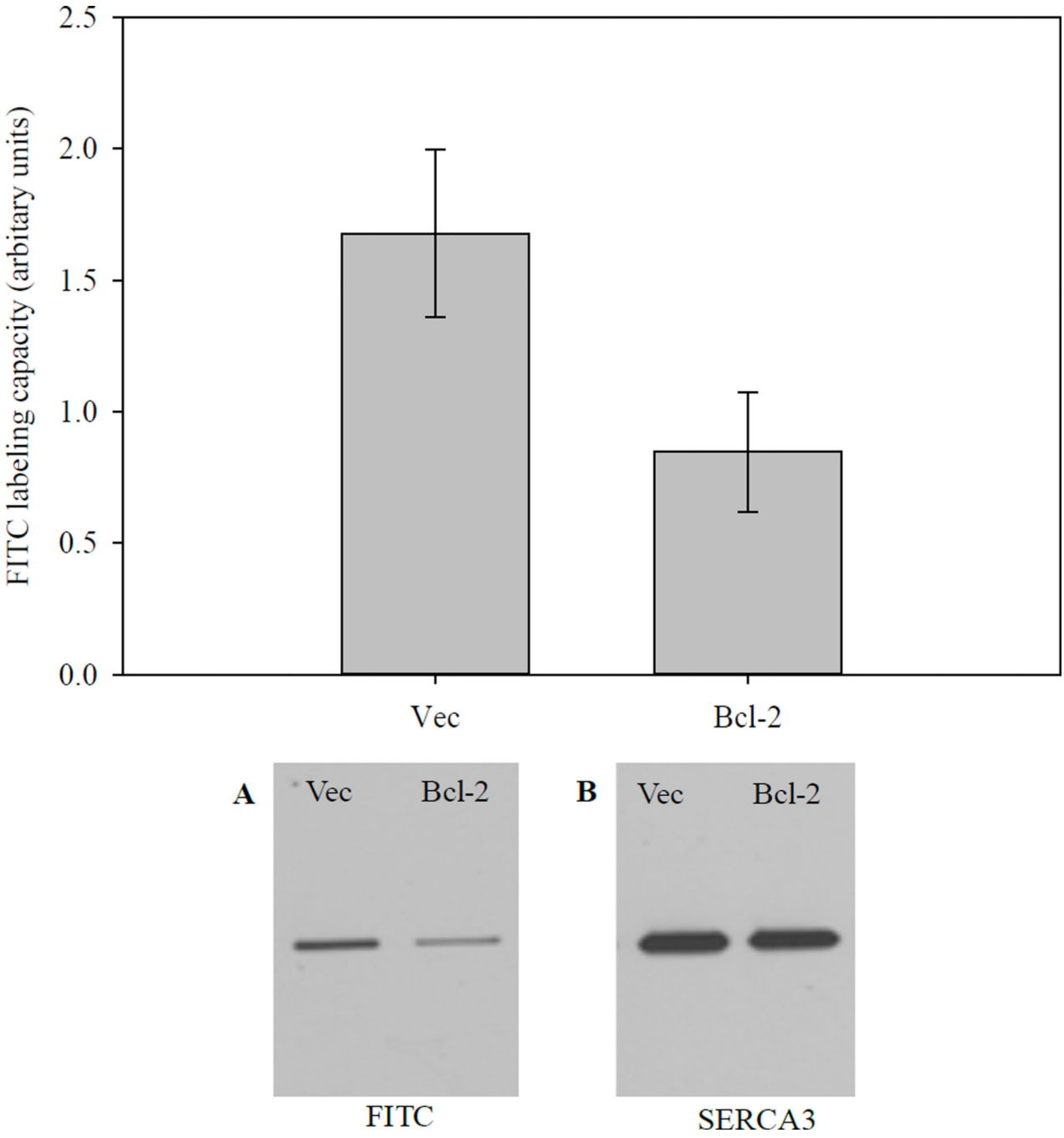

Figure 8. FITC labeling of SERCA

Top: Microsomes isolated from HEK-293 cells transfected with a cDNA construct without the sequence for Bcl-2 (Vec) and microsomes isolated from HEK-293 cells transfected with a Bcl-2-encoding vector (Bcl-2) were labeled with FITC followed by densitometry. The graph shows a summary of six experiments after normalizing to the amount of SERCA3b present in each sample. ***Bottom:*** A representative western blot showing FITC labeling of SERCA3b in Vec and Bcl-2 samples **(A)**. The amount of SERCA3b in each sample is also shown **(B)**.

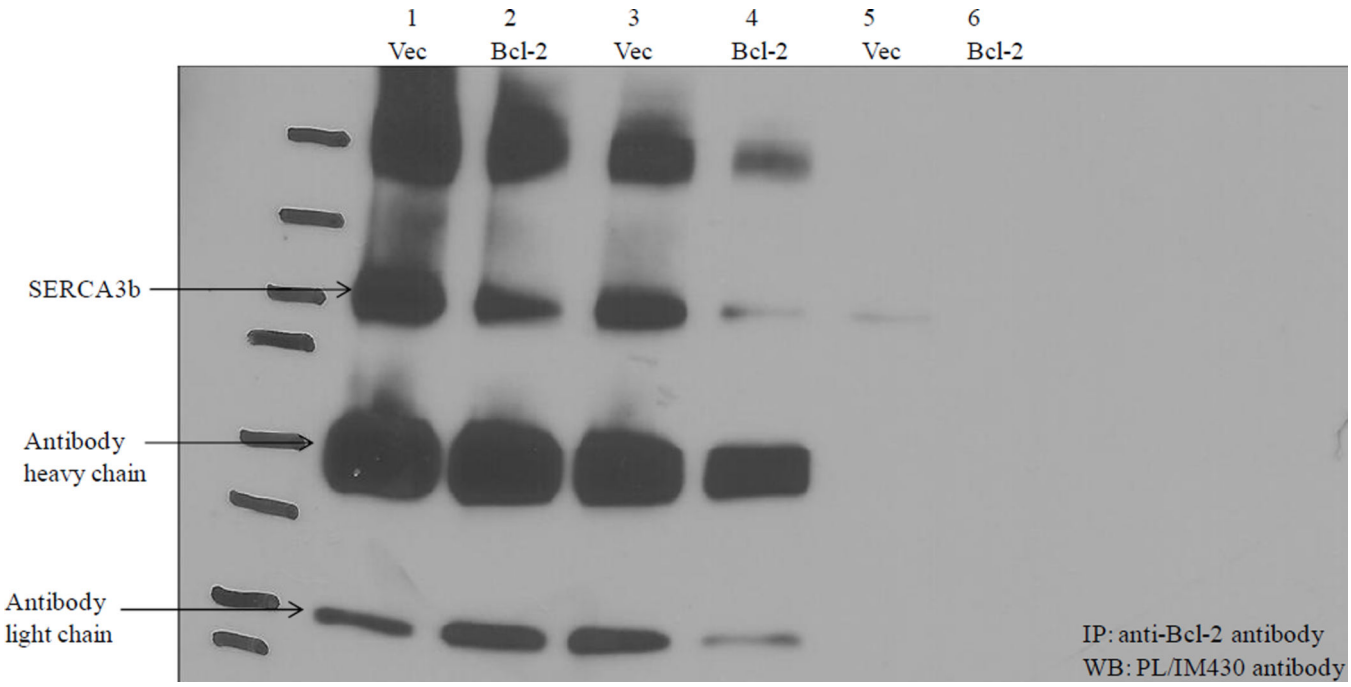

Figure 9. Co-immunoprecipitation of SERCA3b with Bcl-2

Co-immunoprecipitation was carried out using microsomes of HEK-293 cells overexpressing SERCA3b (Vec) and microsomes of HEK-293 cells overexpressing SERCA3b and Bcl-2 (Bcl-2) with the anti-Bcl-2 antibody followed by Western blotting with PL/IM430 antibody. Data from two different microsome isolations (first and second) are shown. Lane 1 and 2 show the first experiment and Lane 3, 4, 5 and 6 show the second experiment. Lane 5 and 6 show control samples run without the anti-Bcl-2 antibody.